Ablation instability experimentally observed on the thin foil metal target surface during its irradiation by terawatt laser

M. Krupka[2,1,3], J. Krása[2], S. Singh[1,2], J. Dostál[1,2], R. Dudžák[1,2], T. Burian[1,2], M. Kálal[3,2], M. Pfeifer[1,2], J. Cikhardt[4,2], D. Klír[4], K. Řezáč[4], T. Pisarczyk[5], T. Chodukowski[5], Z. Rusiniak[5], M. Krůs[2] and L. Juha[1]

[1] *Institute of Physics of the Czech Academy of Sciences, Prague, Czech Republic*

[2] *Institute of Plasma Physics of the Czech Academy of Sciences, Prague, Czech Republic*

[3] *Faculty of Nuclear Sciences and Physical Engineering, Czech Technical University in Prague, Czech Republic*

[4] *Faculty of Electrical Engineering, Czech Technical University in Prague, Czech Republic*

[5] *Institute of Plasma Physics and Laser Microfusion, Warsaw, Poland*

Abstract

Time evolution of plasma density modulations in case of thin foil metal targets was observed during the irradiation with focused terawatt iodine PALS laser beam. These modulations were simultaneously recorded using femtosecond interferometry in three time frames and x-ray streak camera allowing to determine growth and decay rates of hydrodynamic instabilities. These modulations were observed during the laser-plasma interaction, in particular several hundred picoseconds before its maximum intensity. Hot electron emission characteristics were measured and analyzed using an angular array of electron spectrometers. Weaker emission of hot electrons from the lead plasma was observed in comparison to lower Z materials.

Introduction

The interaction of laser radiation with solid matter at intensities above 10^{15} Wcm^{-2} gives rise to ionization of matter, creating plasma on the surface of the target and leads to production of accelerated particles and x-ray photons. [1] The laser produced plasma is also a considerable source of electromagnetic pulses. [2] In this paper we present the results of interferometric measurement of time evolution of laser produced plasmas on thin metal foils (Pb, Zn). The thin metal foils were irradiated using high power iodine laser (1315 nm) by energies between 400-600 Joules with pulse length of 400 ps, reaching intensities up to $3 \cdot 10^{16}$ W $\cdot$ cm^{-2} in the focus. The femtosecond Titanium sapphire laser system is precisely synchronized to the main iodine system to allow precise control of interferometric probe beam timing. [3] These measurements were conducted as a part of the investigation of mechanisms of ion acceleration and electromagnetic pulse generation, where the spatio-temporal ion emission and electromagnetic pulse characteristics were investigated. [4, 5]

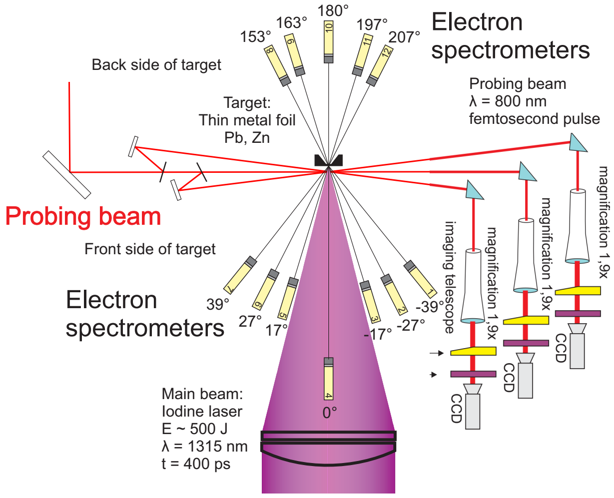

Figure 1: *Outline of the experimentals setup, showing the positions and orientation of electron spectrometers, as well as the 3-frame interferometric diagnostic system. X-ray streak camera is positioned from the top.*

The laser produced plasma electron density distribution was measured using the 3 frame interferometer. The delay between the frames was 400 ps. [6] The electron density was obtained using the inverse Abel transform algorithm based on fourier transform decomposition. [7] To investigate the hot electron emission characteristics the multichannel angular array of electron spectrometers was used. Seven spectrometers were placed in the front side of the target and five were placed in the back side of the target. The energy range covered by the spectrometers was from 50 keV to 1.5 MeV. [8]

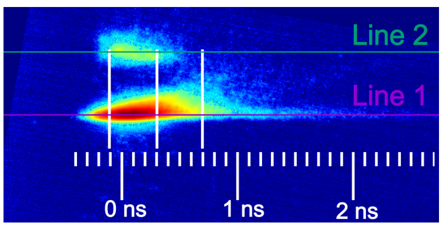

(a) Streak camera image

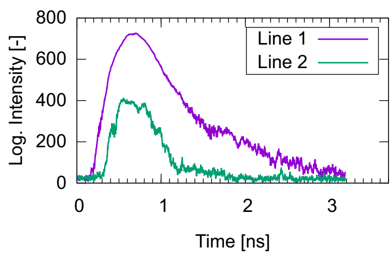

(b) Lineout of the intensity in time.

Figure 2: *Time evolution of x-ray emission of the laser produced plasma on the lead target (shot 53317). The snapshots of interferometric images are denoted by the vertical white lines and lineouts are denoted by horizontal lines.*

Experimental results

Thin lead and zinc foils with a thickness of 6 μm and 2.5 μm, respectively, were used as targets. Spatial distribution of electron plasma density was obtained using the interferometers. The spatial distributions of plasma on the front side of the target are shown in figure 3 for lead target (a-c) and zinc target (d-f). The temporal evolution of x-ray emission for lead target is also shown in figure 2 where the horizontal axis shows a with denoted time frames of interferometric images of electron density. The x-ray emission is imaged in direction along the laser axis, which is shown in vertical direction on the streaked image. Both streak images and framed interferometric images show modulations along the laser axis. These modulations were observed for other shots with thin lead foil targets with different intensities.

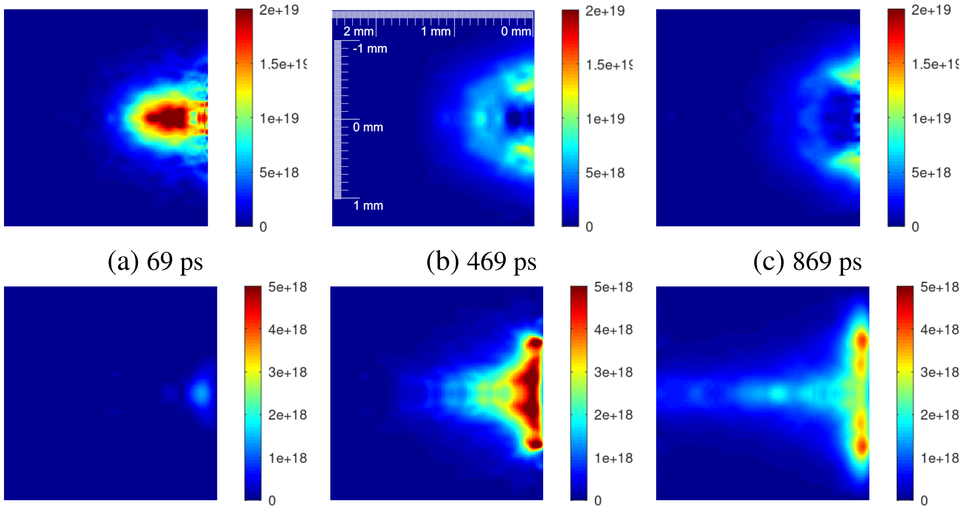

(a) 69 ps (b) 469 ps (c) 869 ps

(d) -468 ps (e) -68 ps (f) 332 ps

Figure 3: *Spatial distribution for electron density for lead target (a,b,c) (shot 53317, energy 497.4 J) and for zinc target (d,e,f) (shot 53386, energy 414.7 J) with delays in regard to the peak of the main laser beam. Electron density is in* cm^{-3}. *Laser radiation comes from the left.*

As a part of the observation of interaction of laser light with thin foil metal targets, the multi channel electron spectrometer array was used and the results are shown in figure 4. The electron energy distribution functions show an almost exponential dependence on energy. The values of hot electron temperatures using exponential fitting are in agreement with the empirical scaling laws. [9] The hot electron emission characteristics show directional emission in the front side of the target (Fig. 4 b,c) and no angular dependence on the back side (Fig. 4 e,f). The angular distribution of hot electron temperature follows the similar pattern as angular density of flux.

Conclusion

The growth and decay of plasma density modulations was observed on the front of the thin foil metal targets by imaging the x-ray emission along the laser axis. These modulations were also observed using the interferometric frames. Given the dynamics of plasma density distributions, the measurement of magnetic fields and electric currents in the plasma using

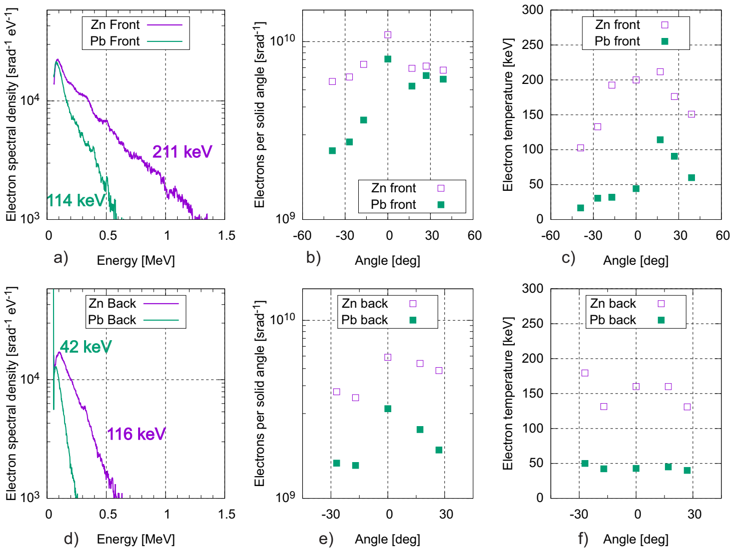

Figure 4: *Characteristics of hot electron emission for lead (shot 53384, energy 420.4 J) and zinc (shot 53386, energy 414.7 J) targets with respect to front (a,b,c) and back (d,e,f) side of the target.*

complex interferometry is required to further investigate the conditions for ion acceleration and electromagnetic pulse generation.

Our observations of hot electron emission characteristics show directional dependence on the front side of the target while the back side of the target shows isotropic pattern of emission. Further investigation into the dependence of hot electron emission characteristics on the target properties is required.

Acknowledgements

The research presented in this paper was supported by the Access to the PALS RI under the EU LASERLAB IV project (Grant Agreement No. 654148), by the Czech Republic's Ministry of Education, Youth and Sports - the projects: Prague Asterix Laser System (LM2015083, LM2018114) and Creating and probing dense plasmas at the PALS facility (CZ.02.1.01/0.0/0.0/16_013/0001552). The research leading to these results has received funding from the Czech Science Foundation (Grant No. 19-02545S and 19-24619S). The support of CTU student support project "Research on optical (nano) structures and laser plasma" SGS19/192/OHK4/3T/14 is gratefully acknowledged as well as the support by the Ministry of Science and Higher Education, Republic of Poland (Decision No. 3880/H2020/2018/2). This scientific work was partly supported by the Polish Ministry of Science and Higher Education within the framework of the scientific financial resources in the year 2020 allocated for the realization of the international co-financed project No.5118/H2020/EURATOM/2020/2. This work has been carried out within the framework of the EUROfusion Consortium and has received funding from the Euratom research and training programme 2014-2018 and 2019-2020 under grant agreement No 633053. The views and opinions expressed herein do not necessarily reflect those of the European Commission.

References

[1] R. S. Craxton *et al.*, Physics of Plasmas **22** (2015) 110501
[2] J. Krása *et al.*, Physics of Plasmas **25** (2018) 113112
[3] J. Dostal *et al.*, Review of Scientific Instruments **88** (2017) 045109
[4] J. Krása *et al.*, Laser and Particle Beams **32** (2014) 15–20
[5] J. Krása *et al.*, Plasma Physics and Controlled Fusion **59** (2017) 065007
[6] T. Pisarczyk *et al.*, Physics of Plasmas **24** (2017) 102711
[7] M. Kalal, K. Nugent, Applied optics **27** 10 (1988): 1956-1959.
[8] M. Krupka *et al.*, Review of Scientific Instruments **92** (2021) 023514
[9] T. Kluge *et al.*, Physical review letters **107** (2011) 205003